Friction and Dimensional Integrity of in-House Fully-Customizable 3D Printed Orthodontic Brackets

2023 Research Aid Awards (RAA)

Dr John Anthony Baker

bakerjohn42@live.com
O: 631-566-4542

FollowUp Form

Award Information

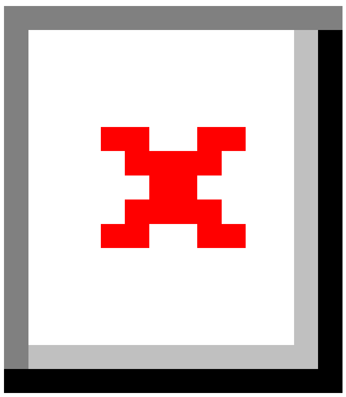

In an attempt to make things a little easier for the reviewer who will read this report, please consider these two questions before this is sent for review:

- *Is this an example of your very best work, in that it provides sufficient explanation and justification, and is something otherwise worthy of publication? (We do publish the Final Report on our website, so this does need to be complete and polished.)*
- *Does this Final Report provide the level of detail, etc. that you would expect, if you were the reviewer?*

Title of Project:*

Friction and Dimensional Integrity of in-House Fully-Customizable 3D Printed Orthodontic Brackets

Award Type

Research Aid Award (RAA)

Period of AAOF Support
July 1, 2023 through June 30, 2024

Institution
University at Buffalo

Names of principal advisor(s) / mentor(s), co-investigator(s) and consultant(s)
Ashish Gurav, David Covell, Steven Makowka

Amount of Funding
$6,000.00

Abstract
(add specific directions for each type here)

See upload

Respond to the following questions:

Detailed results and inferences:*
If the work has been published, please attach a pdf of manuscript below by clicking "Upload a file".
OR
Use the text box below to describe in detail the results of your study. The intent is to share the knowledge you have generated with the AAOF and orthodontic community specifically and other who may benefit from your study. Table, Figures, Statistical Analysis, and interpretation of results should also be attached by clicking "Upload a file".

JAB Supporting Tables and Figures - Reduced Document Size.pdf
Described below is an excerpt from my thesis (currently unpublished), with attached supporting tables and figures.

Results:

Pilot Testing:
Initial pilot testing revealed that brackets of typical industrial size printed with the long axis 45 degrees to the build platform do not yield model prints with enough natural support to survive 3D-printing without internal supports or break-away supports in critical areas, such as the underside of the tie wings or inside the slot. Since it is mandatory that the slot remain as true to STL dimensions as possible, we ultimately decided to print the final brackets with the base of the slot oriented parallel to the build platform, contrasting with the literature.

When printed 1:1 with the STL file without dimensional modification, pilot measurement data revealed a resultant print slot dimension of about 0.0185" after post-processing, indicating that a multiplicative scaler was necessary to account for polymerization shrinkage. To achieve a post-processing inciso-gingival slot dimension equivalent to that of the esthetic control, the proportionality constant was determined to be 1.1765. Thus, manufacturing methods were modified accordingly.

Various STL models were experimented with during pilot testing, including Dentaurum Discovery Pearl and Equilibrium 2 as well as a new STL created by scanning an existing maxillary right canine bracket with 0.022" slot and 0° torque (3M Victory Series, 3M). Ultimately, it was determined that the Dentaurum Discovery Pearl STL was the strongest of the three in terms of structural integrity of the 3D-prints, and the other two experienced a high incidence of fracture at stress concentrations along the slot corners (Figure 15).

Pre-test Measurements:

Pre-test measurements revealed that the inciso-gingival slot dimension of the metal brackets specified by the manufacturers as 0.022" measured as a mean of 0.021" (σ=0.001). The ceramic brackets mean inciso-gingival slot dimension was 0.023". The final VSC inciso-gingival slot dimensions averaged 0.024 (σ=0.001) (Table 2). There was the highest variability within the 3D-printed VSC groups, when compared to the injection molded metal and ceramic, best observed with graphic representation (Figures 16, 17). The different sub-groups for friction testing consisted of randomly selected brackets, and there were no significant differences in initial IG Height between sub-groups using the same bracket material. (Table 3). However, when inter-material comparisons were made, it was revealed that brackets of different material had different IG Heights. For example, brackets made of metal had different IG Height than brackets made of ceramic, and so on (Table 4). To summarize, pre-test measurements revealed matched sub-groups; Metal, ceramic, and VSC brackets did not have matched slot IG height when comparing between bracket material.

There were significant differences in pre-test slot wall angulations between bracket types (Table 5). It should be noted that this data did not have a normal distribution, so limited conclusions may be drawn. The metal and ceramic bracket wall angulations were statistically similar in the steel wire sub-groups, but statistically different in the NiTi subgroups (Table 6). Additionally, the ceramic and VSC bracket wall angulations were similar in the NiTi groups (Table 6). All other bracket and wire combinations showed statistical differences in slot wall angulation (Table 6). Because of the transformations to the data to allow for comparisons to be made, specific conclusions regarding slot angulation magnitude cannot be made. Broadly, mean pre-test slot angles of Metal brackets were slightly obtuse, slot angles of ceramic brackets were near 90 degrees, and slot angles of VSC brackets were slightly acute (Table 2).

Friction Testing:

While SS wires appear initially to produce lower static frictional force than NiTi wires based on mean, statistically, this was not significant (Tables 7A, 7B, 8A2, 8B2). Friction testing yielded no statistically significant differences in static frictional forces between any of the bracket material groups (metal, ceramic, VSC) for first- or second-run (Table 8A1, Table 8B1, Figure 18). Additionally, static friction forces did not differ significantly with contrasting wire materials (SS or NiTi) during the first- or second-run (Table 8A2, Table 8B2, Figure 18). Friction descriptive statistics are displayed in Table 7.

On the third run, there was a significant difference between static frictional force in case of both the metal and VSC groups when contrasting wire materials (Metal-SS vs Metal-NiTi, VSC-SS vs VSC-NiTi), where there was higher static frictional force with NiTi wires in both contrasts (adj $p = 0.017$, 0.014 respectively) (table 8C2, Figure 18). During the third run, the Metal-SS group measured 62.2% of the static friction force of the Metal-NiTi group, and the VSC-SS group measured 59.3% of the static friction force of the VSC-NiTi group.

Static friction force when using SS wires remained generally more consistent than that of NiTi with progressive runs across all bracket material groups (Figure 18D and E).

Post-test Measurements:

For each individual material, there was no statistically significant difference in bracket post-test inciso-gingival slot height when contrasting wire type, except for VSC-NiTi and VSC-SS, where the post-test slot dimension of the VSC-NiTi group was significantly greater than that of VSC-SS group (adj $p = 0.015$) (Table 3). This is consistent with the SEM results, detailed below.

Post-test slot angle deviations showed that there were significant differences in the SS wire groups, but not in the NiTi wire groups between bracket materials (Table 5). Within the SS wire groups, there were significant differences in post-test metal and ceramic slot angulations and metal and VSC angulations (Table 6), where the ceramic bracket slot angles remained closest to 90°, with the metal brackets tending toward divergence, and the VSC brackets tending toward convergence. There was no significant difference in ceramic and VSC post-test slot angulation (Table 6).

Dimensional Stability:

There was no significant difference in post-test and pre-test inciso-gingival slot dimension for any bracket composition when run through friction tests with a stainless-steel wire (Table 9). Additionally, there was no significant dimensional change in the inciso-gingival slot dimension of ceramic brackets after friction tests with NiTi wires (Table 9). In contrast, there was a statistically significant difference in Metal and VSC bracket inciso-gingival slot dimension after friction testing with NiTi wires, where the post-test dimension was greater than that of the pre-test dimension in both groups (Table 9), which is supported by the SEM findings, detailed later (Figure 19).

There were significant changes in slot deviation from before and after friction testing in the metal-SS and metal-NiTi groups, where the post-test angles diverged farther from 90 degrees in the SS subgroup and converged closer to 90 degrees in the NiTi group (Tables 2, 10). All other bracket and wire combinations did not show significant change in maximal slot deviation (Table 10).

Reliability:

Repeated measures for inciso-gingival slot height revealed an intra-rater correlation coefficient (ICC) of 0.855, [CI = 0.674, 0.939], which suggests good reliability (Table 12). Repeated measures for slot angulations revealed an ICC of 0.496, [CI = 0.224, 0.697], which is indicative of poor reliability.

Scanning Electron Microscopy:

Scanning electron microscopy revealed that there was some material transfer of stainless steel onto the ceramic bracket surface from the SS wire that passed through it. Although the bracket slots of VSC were discolored, there was no material transfer observed. However, there was a unique finding in each of the VSC bracket/wire combinations in that the wire's passage through the slot eliminated any gross irregularity within it, effectively polishing the surface and slightly widening the slot (Figure 19).

Aside from this, mechanical changes included the NiTi wire scratching the metal bracket that it passed through. All other bracket and wire combinations were unremarkable. Each wire face that contacted the slot was unchanged (Figure 19).

Material composition of the VSC was analyzed via energy dispersive X-ray spectroscopy. Within this, there were homogenous zones and filler islands. The filler was determined to be an Aluminum Silicate glass with an added Barium, likely present for opacity. There was also a considerable degree of oxygen absorption (Figure 20).

Conclusions:

1. VSC brackets can be 3D-printed within acceptable dimensional tolerances.
2. VSC brackets modeled after Dentuarum Discovery Pearl STL are suitable from a sliding mechanics perspective, but not from a durability perspective.
3. VSC bracket STL design, scaling and post-processing must be further refined for use from both slot precision and durability perspectives.
4. VSC brackets have comparable frictional properties to metal and ceramic injection molded brackets when ligated with stainless steel ligatures on both stainless steel and NiTi wires.
5. VSC brackets can withstand sliding mechanics without significant wear.

Were the original, specific aims of the proposal realized?*
The original specific aims were realized. Our results suggest that in-house 3D-printed orthodontic brackets made of VSC have similar frictional properties and slot dimensional integrity to injection-molded metal and ceramic brackets when tested with stainless-steel and nickel-titanium archwires in-vitro.

Were the results published?*
No

Have the results of this proposal been presented?*
Yes

To what extent have you used, or how do you intend to use, AAOF funding to further your career?*
I have used AAOF funding to complete my thesis project for the Master of Science Degree in Orthodontics. The AAOF has provided an excellent launch for an innovative career.

Comment: *The AAOF thanks you for the completion of your project and your contribution to advancing the orthodontic specialty. We encourage you to pursue the publication of your results and hope that you will pursue AAOF funding in the future.*

Accounting: Were there any leftover funds?
$677.73

Not Published

Are there plans to publish? If not, why not?*
Currently, the thesis has been successfully defended and is undergoing review.
After, it will be consolidated into a manuscript and published in a peer-reviewed orthodontic journal.

Presented

Please list titles, author or co-authors of these presentation/s, year and locations:*
Dimensional Accuracy of in-House 3D-Printed Orthodontic Brackets

John A. Baker, DDS; Ellie Jarvis, BS; Steven Makowka, MS; David Covell, DDS, PhD; Ashish Gurav, DMD, PhD
2024
University at Buffalo Student Research Day 2024

Was AAOF support acknowledged?

If so, please describe:

AAOF support was acknowledged verbally and visually at both my poster presentation at UB Student Research Day 2024 and thesis defense.

Internal Review

Reviewer comments

Reviewer Status*

Approved

File Attachment Summary

Applicant File Uploads

- JAB Supporting Tables and Figures - Reduced Document Size.pdf

Supporting Tables:

Table 2: Bracket Dimension Descriptives

Descriptives: (IG Height in inches, Angle_1 and Angle_2 in degrees, time pre- and post-friction testing)

Wire	Type	Time	variable	n	min	max	median	iqr	mean	sd
SS	Metal	Pre	I_G_Height	16	0.02	0.023	0.021	0.001	0.021	0.001
SS	Metal	Pre	Angle_1	16	88.982	92.306	91.099	1.332	91.099	0.924
SS	Metal	Pre	Angle_2	16	89.092	91.976	90.588	1.107	90.573	0.837
SS	Metal	Post	I_G_Height	16	0.02	0.023	0.021	0.001	0.021	0.001
SS	Metal	Post	Angle_1	16	89.051	96.512	91.664	3.016	91.877	1.985
SS	Metal	Post	Angle_2	16	87.399	97.984	91.7	2.266	92.094	2.43
SS	Ceramic	Pre	I_G_Height	16	0.021	0.024	0.023	0.001	0.023	0.001
SS	Ceramic	Pre	Angle_1	16	89.622	91.941	90.541	0.816	90.682	0.673
SS	Ceramic	Pre	Angle_2	16	89.018	91.782	90.362	1.228	90.487	0.815
SS	Ceramic	Post	I_G_Height	16	0.021	0.023	0.022	0.001	0.022	< 0.001
SS	Ceramic	Post	Angle_1	16	89.375	92.443	90.124	0.347	90.287	0.652
SS	Ceramic	Post	Angle_2	16	89.063	92.344	90.953	1.048	90.985	0.865
SS	VSC	Pre	I_G_Height	16	0.022	0.025	0.023	0.001	0.023	0.001
SS	VSC	Pre	Angle_1	16	87.633	91.82	89.606	1.438	89.753	1.134
SS	VSC	Pre	Angle_2	16	88.535	91.81	89.469	1.507	89.789	1.022
SS	VSC	Post	I_G_Height	16	0.022	0.025	0.024	0.001	0.024	0.001
SS	VSC	Post	Angle_1	16	86.07	97	89.306	1.256	89.451	2.439
SS	VSC	Post	Angle_2	16	87.99	94.486	90.162	1.754	90.229	1.572
NiTi	Metal	Pre	I_G_Height	16	0.02	0.021	0.021	0.001	0.021	< 0.001
NiTi	Metal	Pre	Angle_1	16	90.448	93.011	91.473	0.876	91.474	0.736
NiTi	Metal	Pre	Angle_2	16	89.193	93.231	91.226	1.428	91.262	1.045
NiTi	Metal	Post	I_G_Height	16	0.02	0.022	0.021	< 0.001	0.021	< 0.001
NiTi	Metal	Post	Angle_1	16	89.597	92.409	90.775	1.209	90.754	0.897
NiTi	Metal	Post	Angle_2	16	89.157	92.187	90.573	1.506	90.804	0.97
NiTi	Ceramic	Pre	I_G_Height	16	0.021	0.023	0.022	0.001	0.023	0.001
NiTi	Ceramic	Pre	Angle_1	16	89.542	90.935	90.374	0.651	90.27	0.463
NiTi	Ceramic	Pre	Angle_2	16	89.919	91.896	90.767	0.728	90.76	0.574
NiTi	Ceramic	Post	I_G_Height	16	0.021	0.023	0.023	< 0.001	0.023	< 0.001
NiTi	Ceramic	Post	Angle_1	16	88.519	92.162	90.278	1.034	90.386	0.891
NiTi	Ceramic	Post	Angle_2	16	89.326	91.57	90.719	0.71	90.647	0.578
NiTi	VSC	Pre	I_G_Height	16	0.022	0.025	0.024	0.001	0.024	0.001
NiTi	VSC	Pre	Angle_1	16	86.607	91.928	88.493	0.995	88.802	1.282

NiTi	VSC	Pre	Angle_2	16	88.178	91.787	89.506	1.723	89.677	1.056
NiTi	VSC	Post	I_G_Height	16	0.022	0.026	0.025	0.002	0.024	0.001
NiTi	VSC	Post	Angle_1	16	87.562	92.132	89.161	1.215	89.409	1.183
NiTi	VSC	Post	Angle_2	16	86.413	92.743	89.126	3.059	89.351	1.913

Table 3: IG Height Contrasts Between Wires (in)

contrast	Type	Time	estimate	p.value	P adj*
SS - NiTi	Metal	Pre	0.0004	0.093	0.140
SS - NiTi	Ceramic	Pre	0.0001	0.818	0.818
SS - NiTi	VSC	Pre	-0.0003	0.212	0.283
SS - NiTi	Metal	Post	-0.0003	0.251	0.302
SS - NiTi	Ceramic	Post	-0.0006	0.017	0.052
SS - NiTi	VSC	Post	-0.0007	0.004	0.015

*Benjamini-Hochberg adjusted *p*-values to control false discovery rate, significance level set to 0.05

Table 4: IG Height Contrasts between Bracket Materials for Each Wire, Pre-Test (in)

contrast	Wire	Time	estimate	p.value	p.adj*
Metal - Ceramic	SS	Pre	-0.0015	< 0.001	< 0.001
Metal - VSC	SS	Pre	-0.0022	< 0.001	< 0.001
Ceramic - VSC	SS	Pre	-0.0007	0.0065	0.0065
Metal - Ceramic	NiTi	Pre	-0.0019	< 0.001	< 0.001
Metal - VSC	NiTi	Pre	-0.0029	< 0.001	< 0.001
Ceramic - VSC	NiTi	Pre	-0.0010	< 0.001	< 0.001

*Benjamini-Hochberg adjusted *p*-values to control false discovery rate, significance level set to 0.05

Table 5: Slot Wall Angulations Contrast Between All Groups at According to Wire and Time Point

Wire	Time	.y.	groups	p-value*
SS	Pre	Max_Angle	Metal, Ceramic, VSC	0.017
SS	Post	Max_Angle	Metal, Ceramic, VSC	0.007
NiTi	Pre	Max_Angle	Metal, Ceramic, VSC	< 0.001
NiTi	Post	Max_Angle	Metal, Ceramic, VSC	0.132

*Kruskal-Wallis test p-value, significance level set to 0.05

Table 6: Slot Angle Deviation Contrasts

Non-parametric contrasts

Wire	Time	.y.	group1	group2	p-value*	p.adj**
SS	Pre	Max_Angle	Metal	Ceramic	0.82	0.820
SS	Pre	Max_Angle	Metal	VSC	0.01	0.030***
SS	Pre	Max_Angle	Ceramic	VSC	0.019	0.040***
SS	Post	Max_Angle	Metal	Ceramic	0.049	0.091
SS	Post	Max_Angle	Metal	VSC	0.002	0.009***
SS	Post	Max_Angle	Ceramic	VSC	0.256	0.383
NiTi	Pre	Max_Angle	Metal	Ceramic	0.002	0.009
NiTi	Pre	Max_Angle	Metal	VSC	< 0.001	< 0.001***
NiTi	Pre	Max_Angle	Ceramic	VSC	0.173	0.288

*Post hoc Dunn test p-values for significant Kruskal-Wallis tests

**Benjamini-Hochberg adjusted p-values over all contrasts, significance level set to 0.05*

***These tests had groups with nonsignificant Levene test, so assumption of equal variance holds and statements about differences in medians are allowed. (Otherwise, significant tests can only be said to have difference in distribution.)

Table 7: Friction-Testing Descriptives (Friction in N)

7A: Run 1

Wire	Type	variable	n	min	max	median	iqr	mean	sd
SS	Metal	Friction	16	0.99	2.73	1.47	0.55	1.55	0.46
SS	Ceramic	Friction	16	0.90	3.03	1.88	1.01	1.81	0.59
SS	VSC	Friction	16	0.85	2.73	1.77	0.33	1.78	0.48
NiTi	Metal	Friction	16	0.78	5.20	2.27	0.96	2.43	1.05
NiTi	Ceramic	Friction	16	0.40	7.30	1.62	1.17	2.07	1.92
NiTi	VSC	Friction	16	1.21	3.55	1.92	1.03	2.07	0.64

7B: Run 2

Wire	Type	variable	n	min	max	median	iqr	mean	sd
SS	Metal	Friction	16	0.72	3.69	1.68	0.46	1.76	0.67
SS	Ceramic	Friction	16	0.51	3.91	1.89	0.74	1.95	0.73
SS	VSC	Friction	16	1.02	3.76	2.01	0.62	2.07	0.76
NiTi	Metal	Friction	16	1.24	7.95	2.38	1.79	3.13	1.90
NiTi	Ceramic	Friction	16	1.06	7.62	2.16	1.41	2.85	1.99
NiTi	VSC	Friction	16	1.69	7.12	2.99	2.31	3.36	1.82

7C: Run 3

Wire	Type	variable	n	min	max	median	iqr	mean	sd
SS	Metal	Friction	16	0.99	6.14	1.75	0.47	1.96	1.19
SS	Ceramic	Friction	16	1.21	5.00	1.86	0.69	2.00	0.91
SS	VSC	Friction	16	1.21	2.64	1.88	0.54	1.87	0.44
NiTi	Metal	Friction	16	0.88	9.19	2.90	2.74	3.4	2.11
NiTi	Ceramic	Friction	16	1.03	5.84	2.20	2.46	2.73	1.44
NiTi	VSC	Friction	16	1.81	7.57	2.98	1.64	3.46	1.95

Table 8: Friction Comparisons with Ratio (N)

Linear mixed effect model estimated marginal means contrasts (all friction values were log transformed)

8A1: Run 1 Contrasts inter-material

contrast	Wire	Estimate*	Ratio	p.value	P adj**
Metal - Ceramic	SS	-0.140	0.869	0.370	0.519
Metal - VSC	SS	-0.141	0.869	0.367	0.519
Ceramic - VSC	SS	-0.001	0.999	0.996	0.996
Metal - Ceramic	NiTi	0.375	1.456	0.018	0.079
Metal - VSC	NiTi	0.115	1.122	0.460	0.519
Ceramic - VSC	NiTi	-0.260	0.771	0.097	0.292

8A2: Run 1 Contrasts inter-wire

contrast	Type	Estimate*	Ratio	p.value	P adj**
SS - NiTi	Metal	-0.400	0.670	0.012	0.079
SS - NiTi	Ceramic	0.115	1.122	0.461	0.519
SS - NiTi	VSC	-0.145	0.865	0.355	0.519

*Difference in log transformed friction values

**Benjamini-Hochberg adjusted p-values to control false discovery rate within run, significance level set to 0.05

8B1: Run 2 Contrasts Inter-Material

contrast	Wire	Estimate*	Ratio	p.value	P adj**
Metal - Ceramic	SS	-0.090	0.824	0.590	0.792
Metal - VSC	SS	-0.164	0.732	0.326	0.792
Ceramic - VSC	SS	-0.074	0.889	0.656	0.817
Metal - Ceramic	NiTi	0.128	1.327	0.444	0.792
Metal - VSC	NiTi	-0.086	0.800	0.605	0.792
Ceramic - VSC	NiTi	-0.214	0.602	0.201	0.724

8B2: Run 2 Contrasts Inter-Wire

contrast	Type	Estimate*	Ratio	p.value	P adj**
SS - NiTi	Metal	-0.494	0.254	0.004	0.060
SS - NiTi	Ceramic	-0.277	0.409	0.099	0.247
SS - NiTi	VSC	-0.416	0.277	0.014	0.060

*Difference in log transformed friction values

**Benjamini-Hochberg adjusted p-values to control false discovery rate within run, significance level set to 0.05

8C1: Run 3 Contrasts Inter-Material

contrast	Wire	Estimate*	Ratio	p.value	P adj**
Metal - Ceramic	SS	-0.052	0.949	0.746	0.893
Metal - VSC	SS	-0.022	0.979	0.893	0.893
Ceramic - VSC	SS	0.031	1.031	0.849	0.893
Metal - Ceramic	NiTi	0.167	1.182	0.301	0.541
Metal - VSC	NiTi	-0.069	0.933	0.668	0.893
Ceramic - VSC	NiTi	-0.236	0.790	0.145	0.325

8C2: Run 3 Contrasts Inter-Wire

contrast	Type	Estimate*	Ratio	p.value	P adj**
SS - NiTi	Metal	-0.475	0.622	0.004	0.017
SS - NiTi	Ceramic	-0.256	0.774	0.114	0.325
SS - NiTi	VSC	-0.523	0.593	0.002	0.014

*Difference in log transformed friction values

**Benjamini-Hochberg adjusted p-values to control false discovery rate within run, significance level set to 0.05

Table 9: Slot IG Height Dimensional Changes from Friction Testing (in)

IGH Linear mixed effect model estimated marginal means contrasts

contrast	Type	Wire	estimate	p.value	P adj*
Pre - Post	Metal	SS	-0.0001	0.511	0.557
Pre - Post	Ceramic	SS	0.0003	0.028	0.068
Pre - Post	VSC	SS	-0.0003	0.056	0.095
Pre - Post	Metal	NiTi	-0.0008	< 0.001	< 0.001
Pre - Post	Ceramic	NiTi	-0.0003	0.046	0.092
Pre - Post	VSC	NiTi	-0.0007	< 0.001	< 0.001

*Benjamini-Hochberg adjusted *p*-values to control false discovery rate, significance level set to 0.05

Table 10: Slot Angle Changes from Friction Testing

Wire	Type	.y.	group1	group2	p*	p.adj**
SS	Metal	Max_Angle	Pre	Post	0.008	0.029
SS	Ceramic	Max_Angle	Pre	Post	0.562	0.766
SS	VSC	Max_Angle	Pre	Post	0.669	0.797
NiTi	Metal	Max_Angle	Pre	Post	0.013	0.033
NiTi	Ceramic	Max_Angle	Pre	Post	0.737	0.797
NiTi	VSC	Max_Angle	Pre	Post	0.744	0.797

*Wilcoxon signed-rank test p-values

**Benjamini-Hochberg adjusted p-values over all contrasts, significance level set to 0.05

***These tests had groups with nonsignificant Levene test, so assumption of equal variance holds and statements about differences in medians are allowed. (Otherwise, significant tests can only be said to have difference in distribution.)

Table 11: IG Height Changes (in)

contrast	Type	Wire	estimate	p.value	P adj*
Pre - Post	Metal	SS	-0.0001	0.511	0.557
Pre - Post	Ceramic	SS	0.0003	0.028	0.068
Pre - Post	VSC	SS	-0.0003	0.056	0.095
Pre - Post	Metal	NiTi	-0.0008	< 0.001	< 0.001
Pre - Post	Ceramic	NiTi	-0.0003	0.046	0.092
Pre - Post	VSC	NiTi	-0.0007	< 0.001	< 0.001

*Benjamini-Hochberg adjusted *p*-values to control false discovery rate, significance level set to 0.05

Table 12: Intra-Examiner Correlation

Variable	ICC	p-value*	95% Confidence Interval
IG Height	0.855	< 0.001	(0.674, 0.939)
Angles	0.496	< 0.001	(0.224, 0.697)

*significance level set to 0.05

Supporting Figures:

Figure 15: Bracket Failures: Demonstrate a shear line at stress concentrations through the path of least resistance

15A: Broken Bracket 1

15B: Broken Bracket 2

15C: Broken Bracket 3

Figure 15D: Broken Bracket 4

Figure 16: Pre- and Post- Test IG Height Comparisons (NiTi): metal showed significant changes

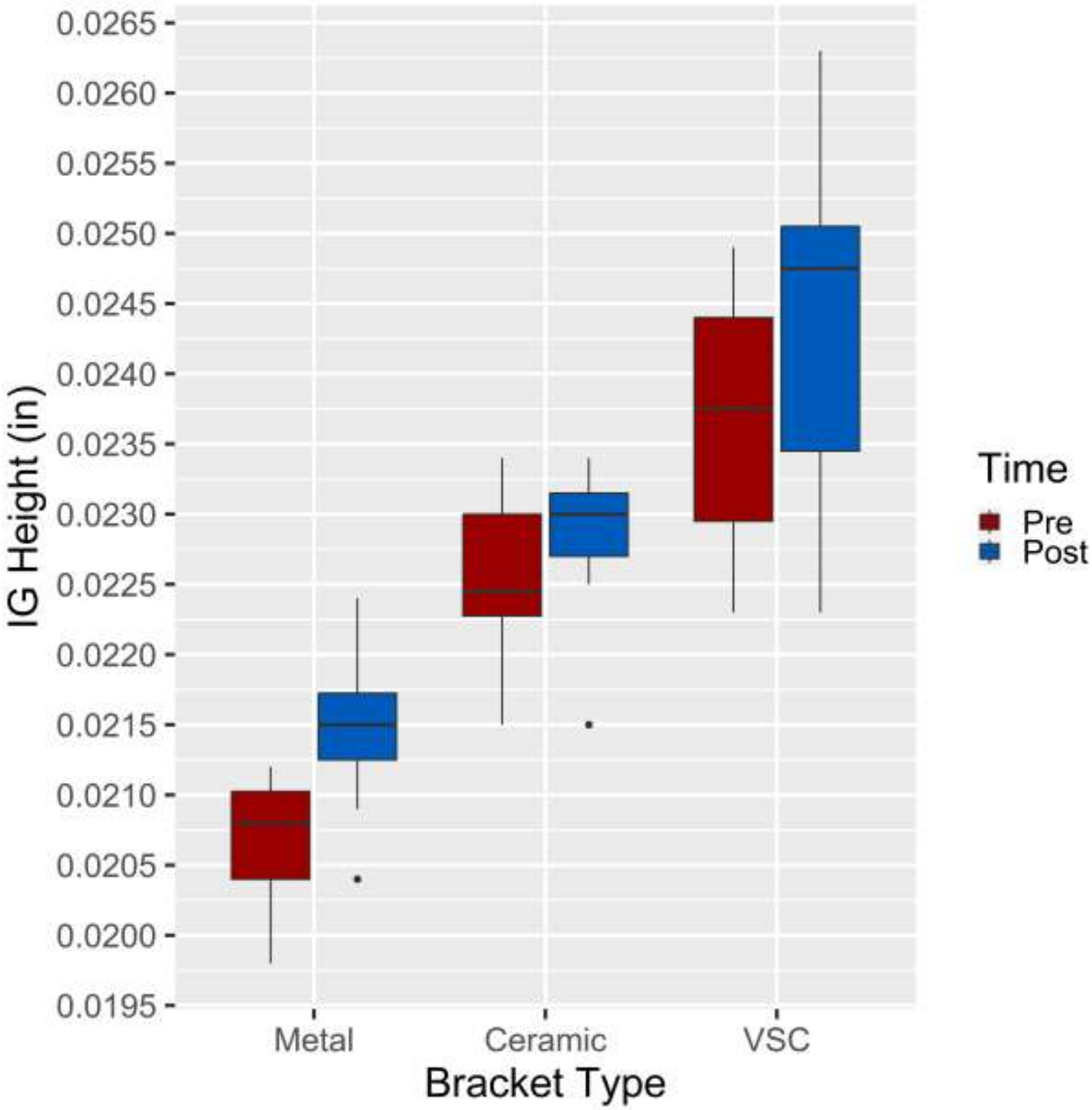

Figure 17: Pre- and Post- Test IG Height Comparisons (SS):

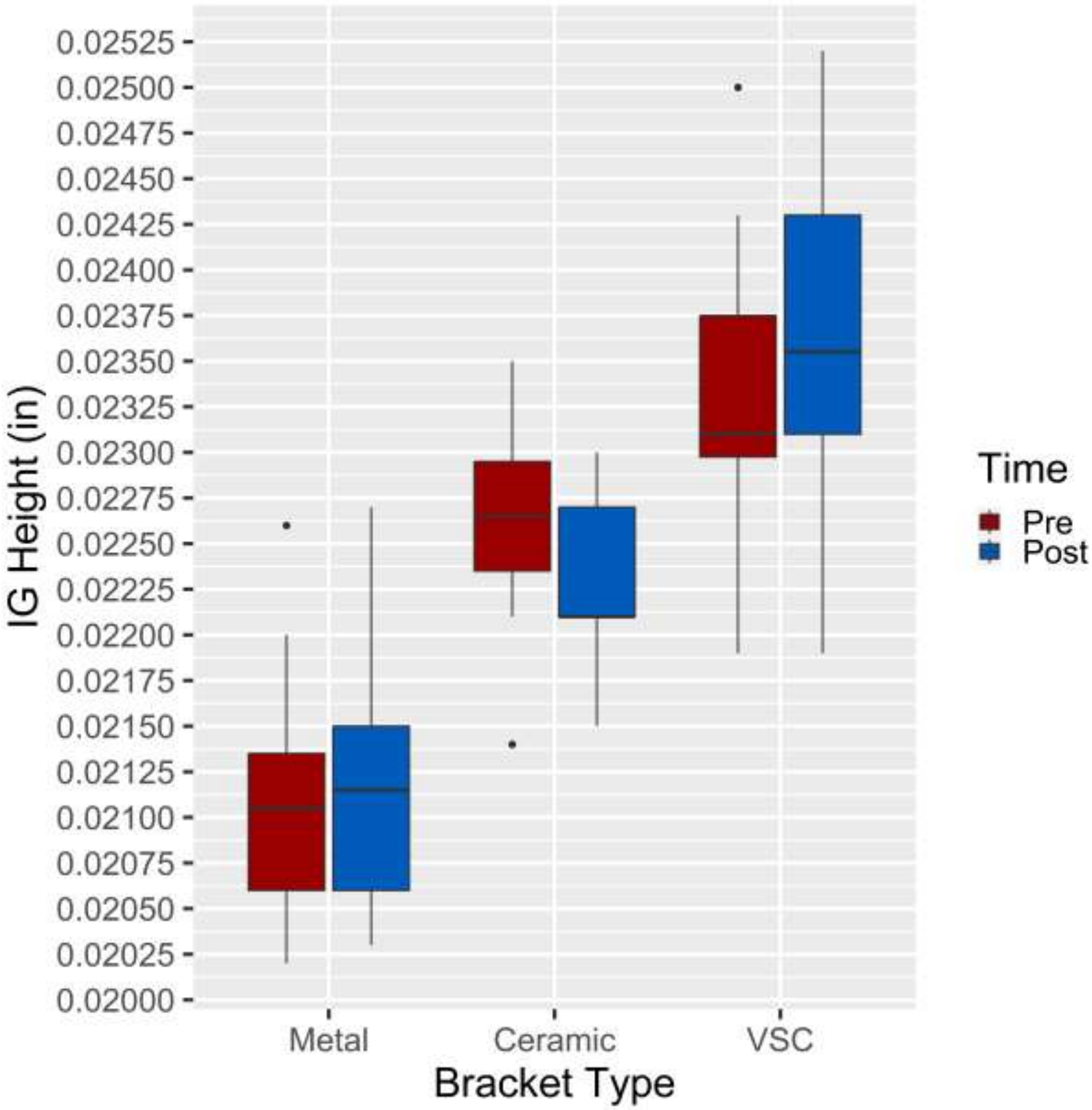

Figure 18: Friction Data

18A: Run 1

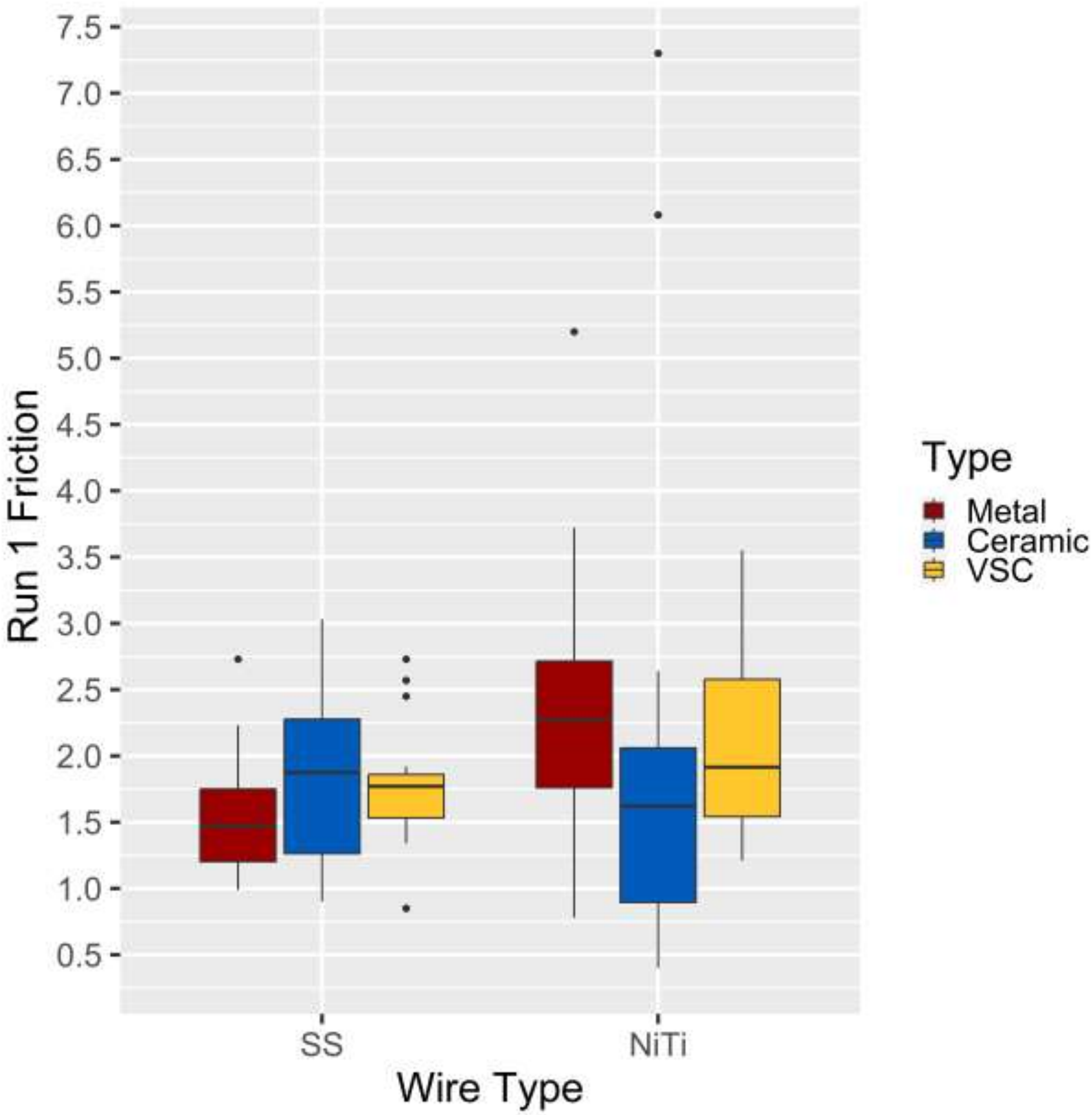

18B: Run 2

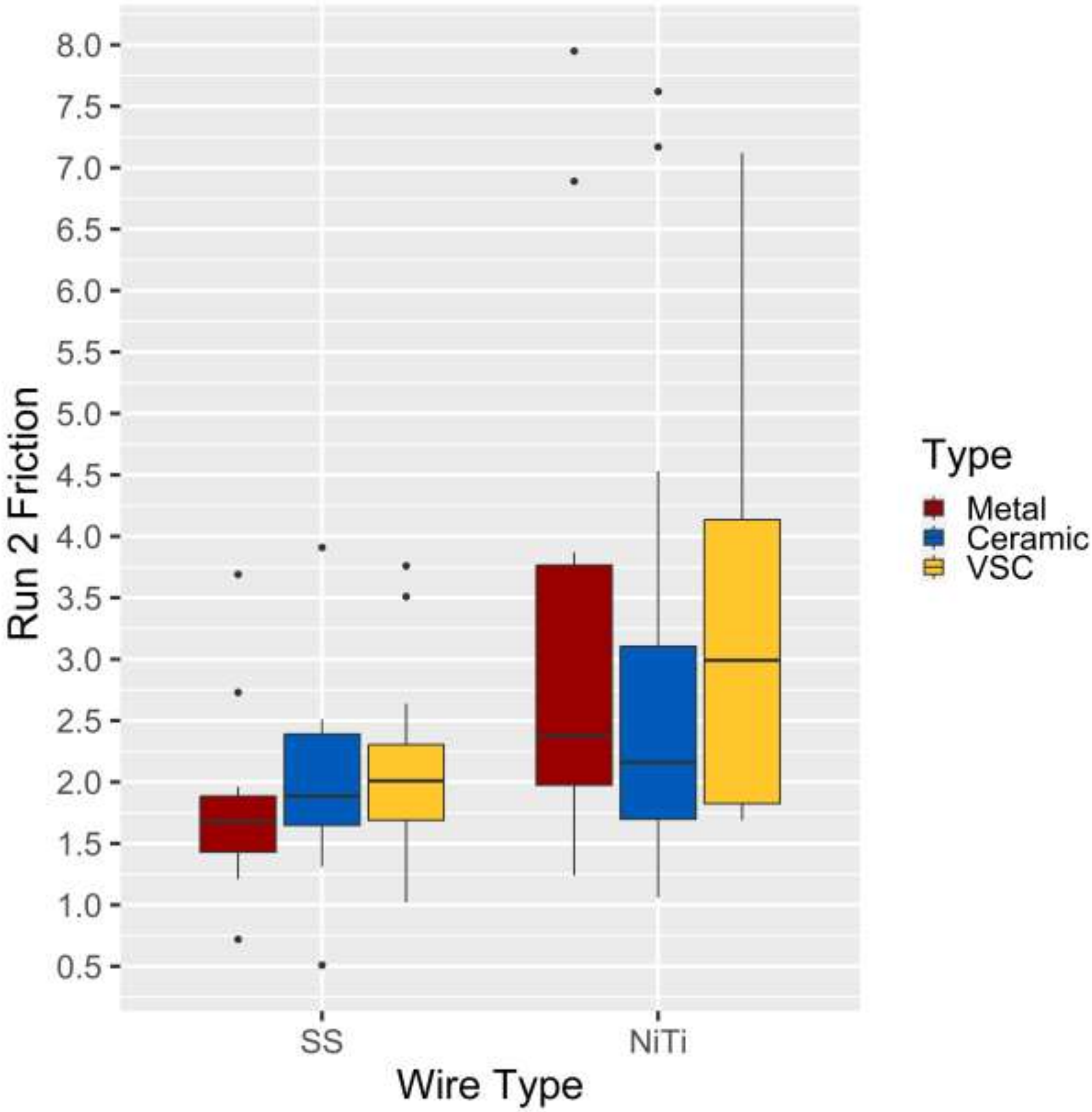

18C: Run 3

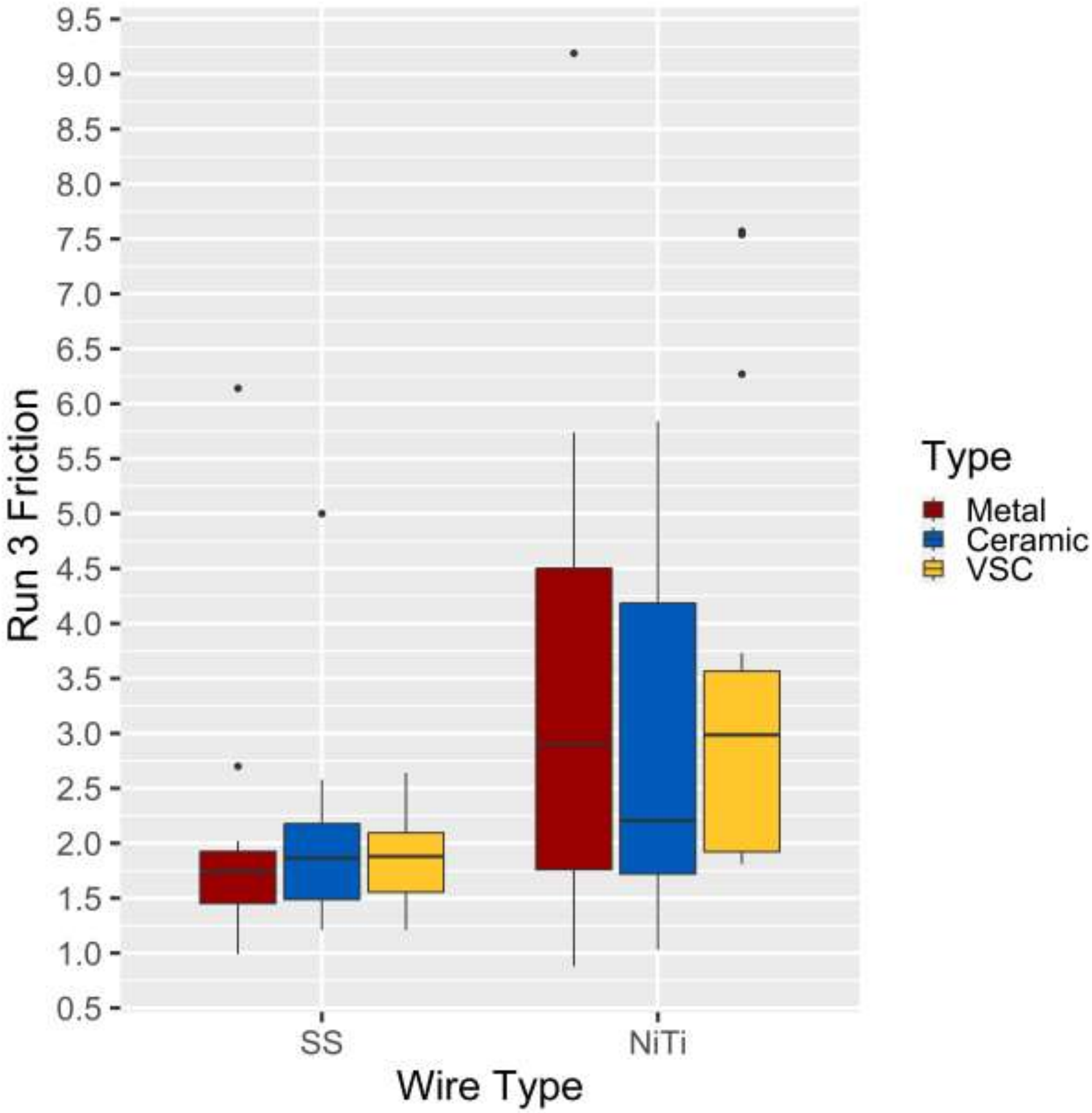

9.5
9.0
8.5
8.0
7.5
7.0
6.5
6.0
5.5
5.0
4.5
4.0
3.5
3.0
2.5
2.0
1.5
1.0
0.5
Run 3 Friction
SS
NiTi
Wire Type
Type
Metal
Ceramic
VSC

18D: All runs (SS)

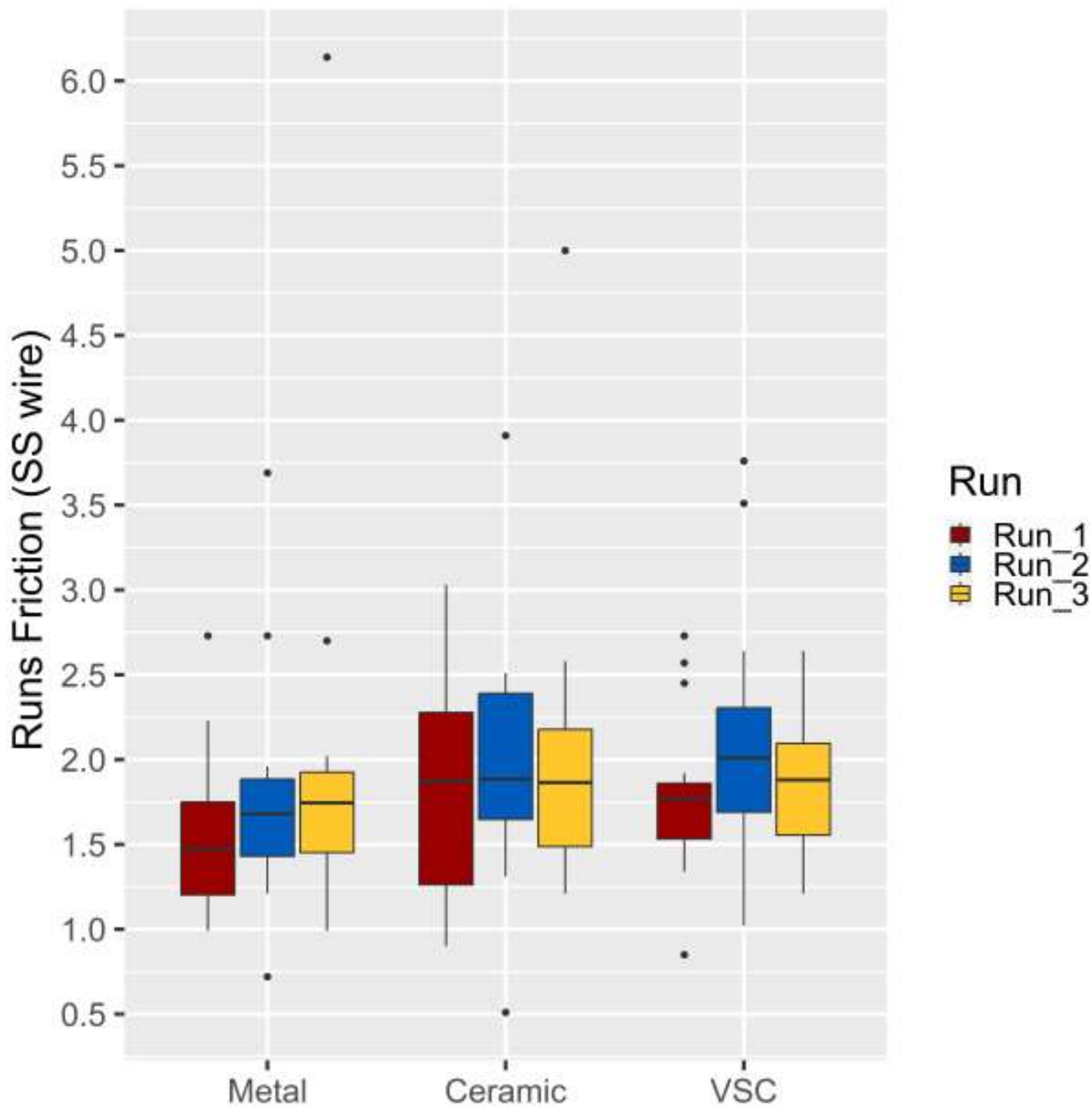

18E: All runs (NiTi): Progressively increasing variability with each run

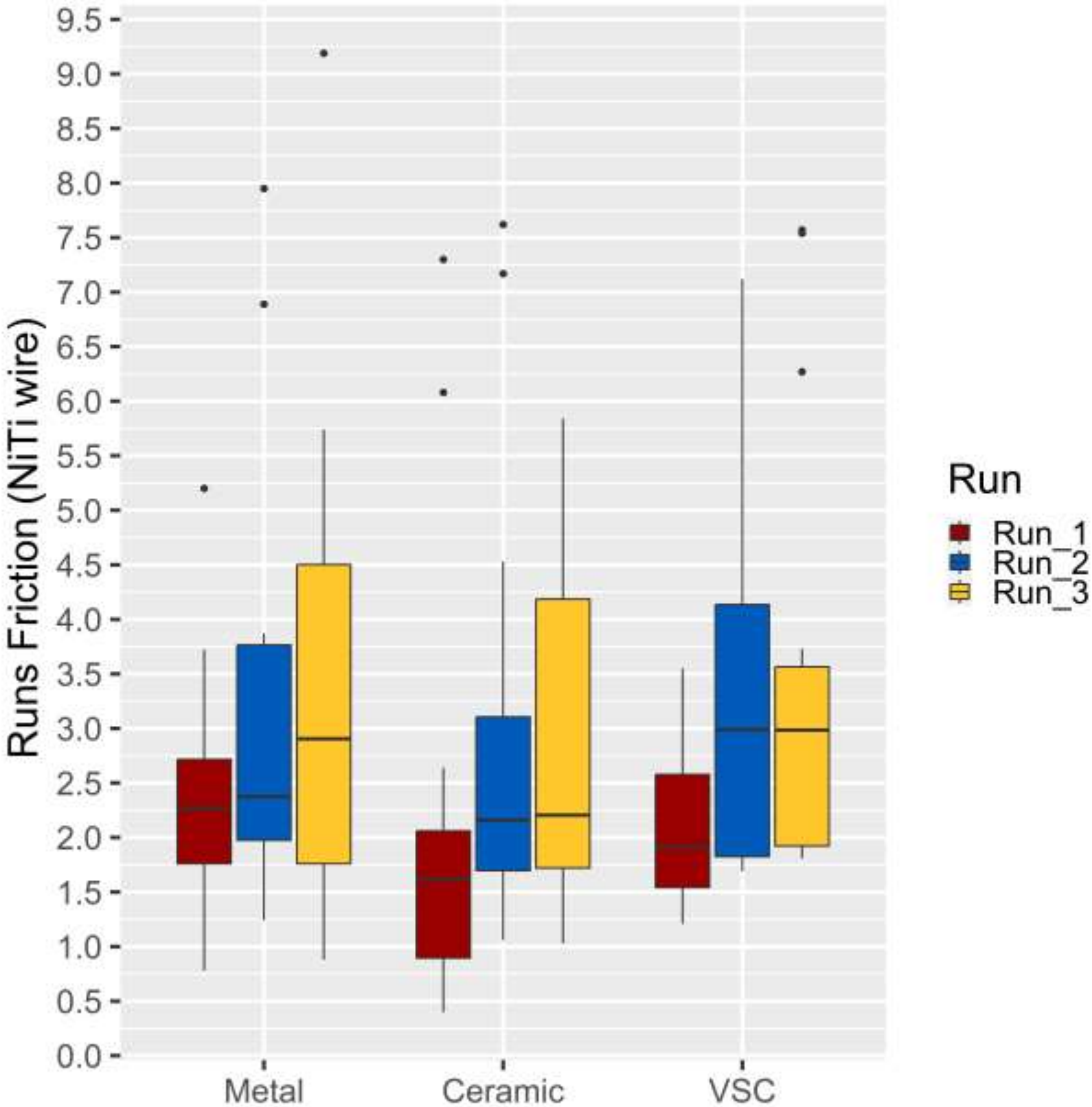

Figure 19: SEM Images

19A: Ceramic-SS: Metal transfer visible, encircled

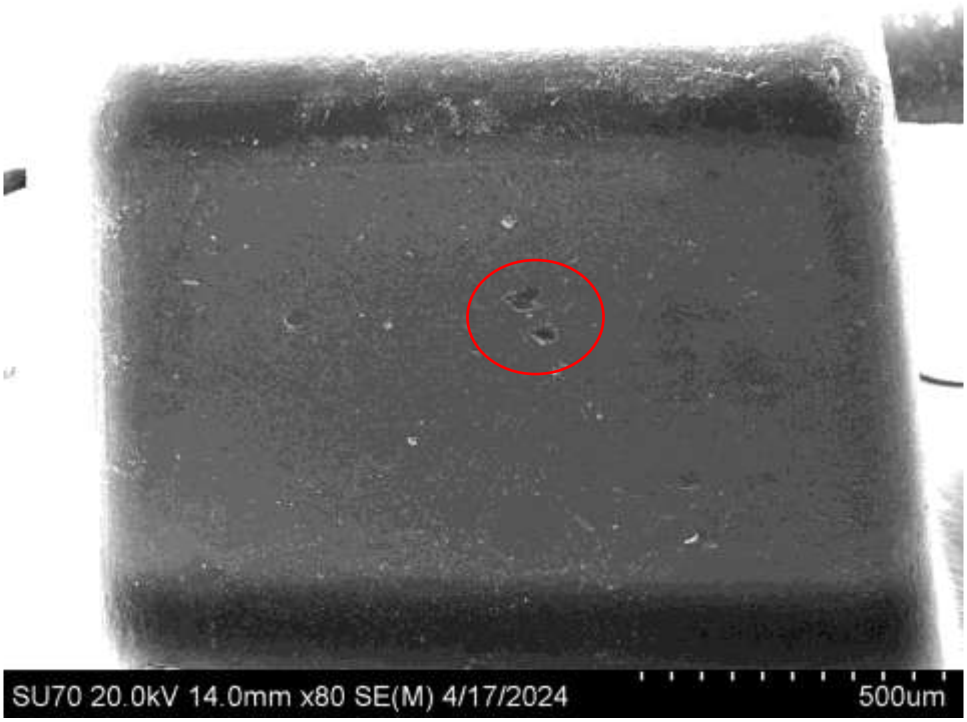

19B: VSC-SS: Area of polish enclosed in red

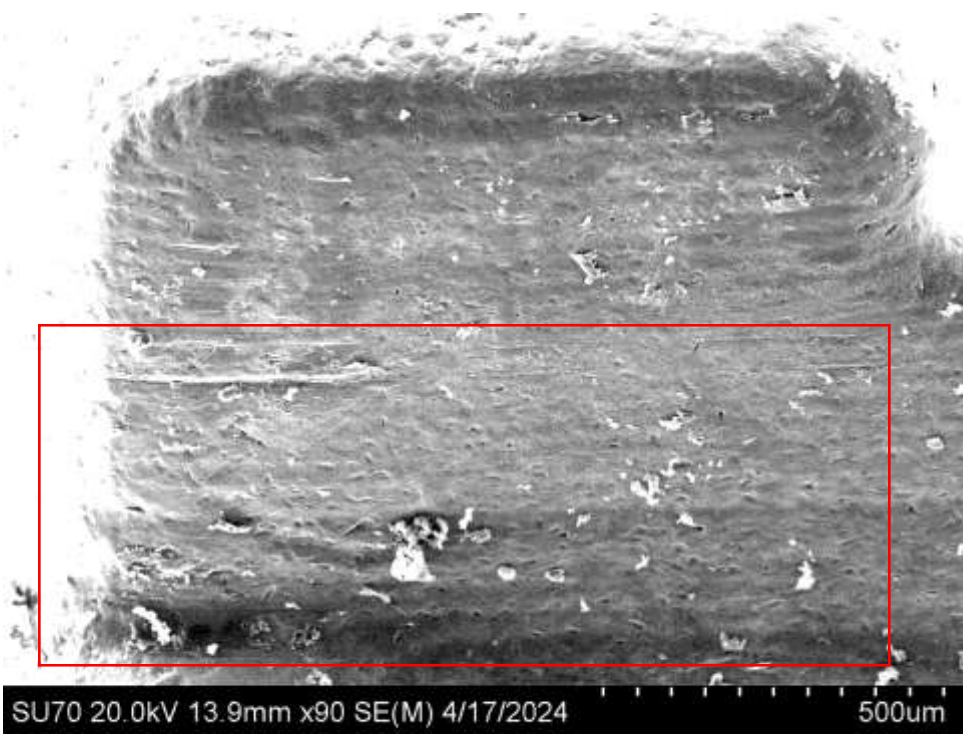

19C: VSC-NiTi: Area of polish enclosed in red

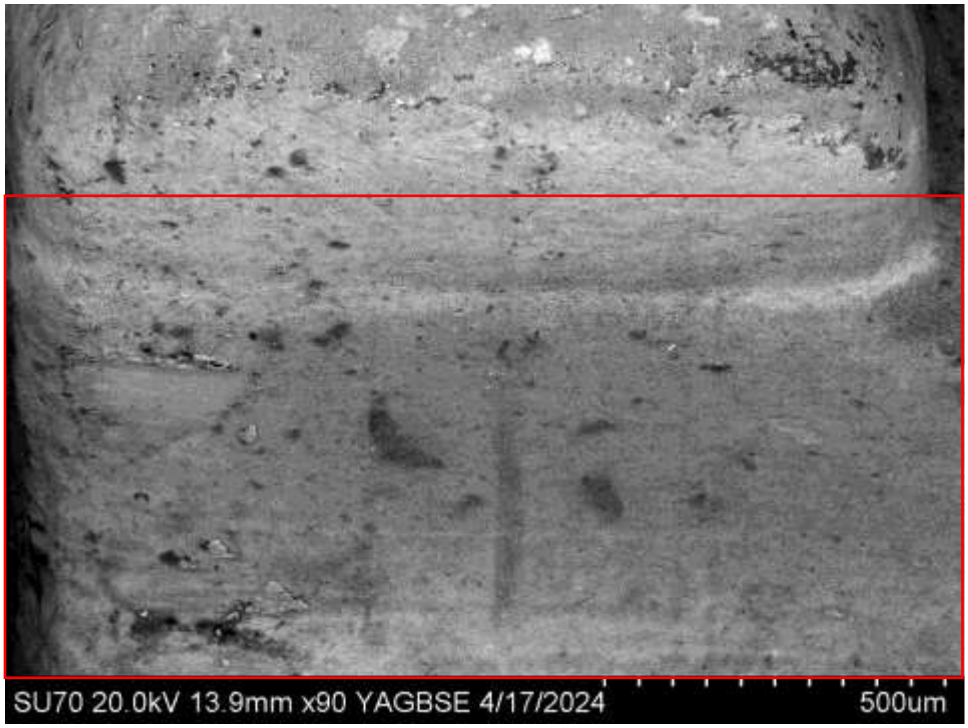

19D: Metal-NiTi: Scratch Encircled

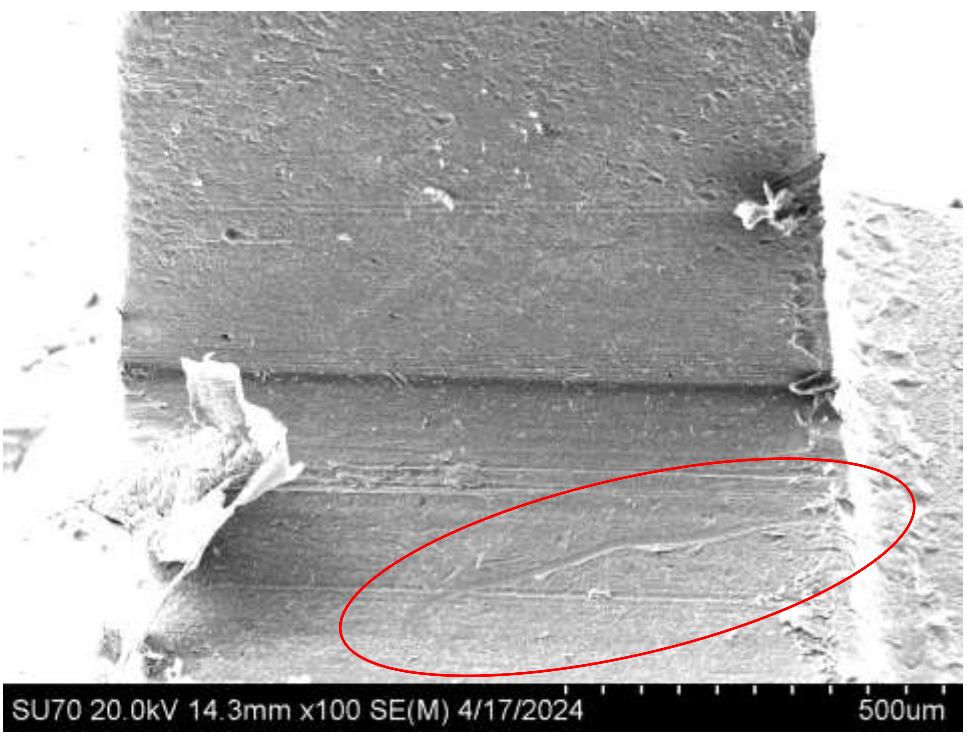

19E: Ceramic-NiTi: unremarkable

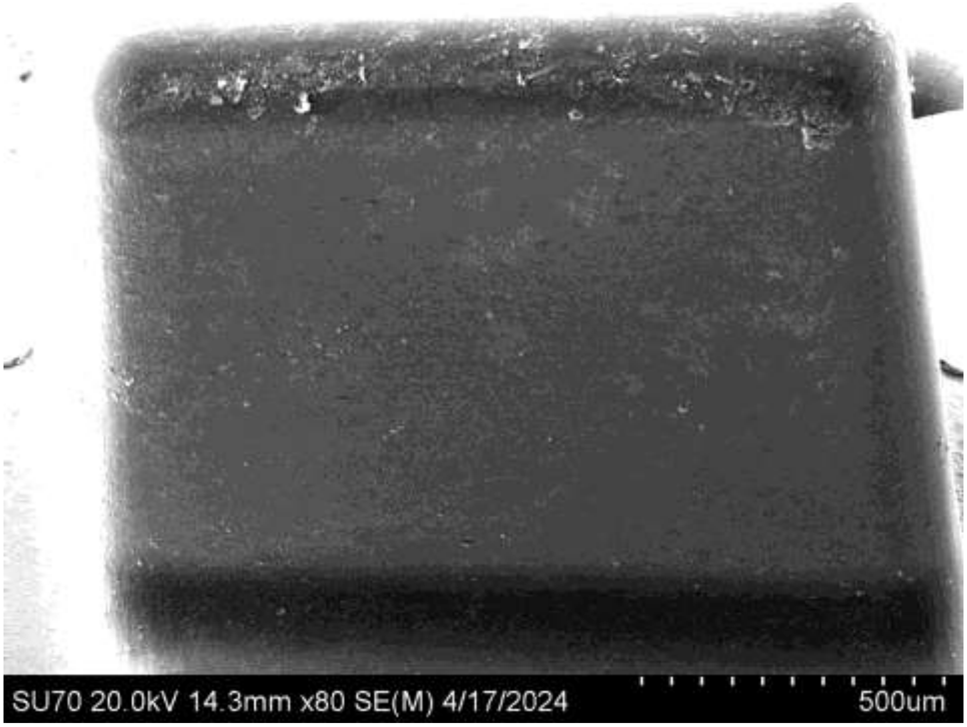

19F: Metal-SS: unremarkable

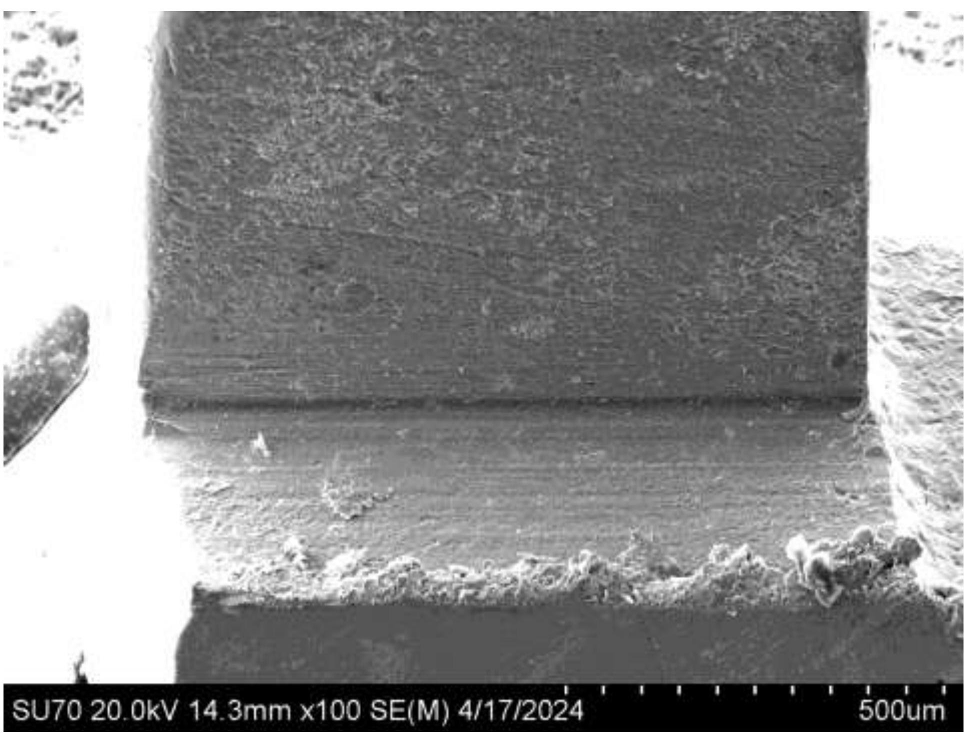

Figure 20: SEM Energy Dispersive X-ray Spectroscopy

20A: SEM – VSC Composition: 1 marks heterogenous zone, 2 marks filler island

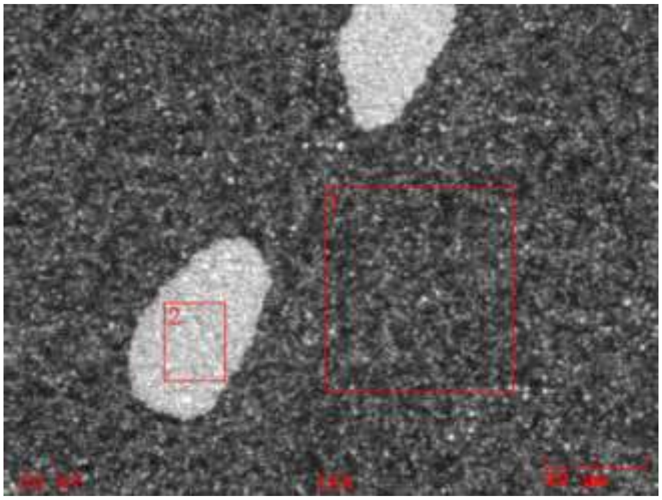

20B: Heterogenous Zone: Peaks represent high concentrations

Analysis Report: BRACKET-1-1

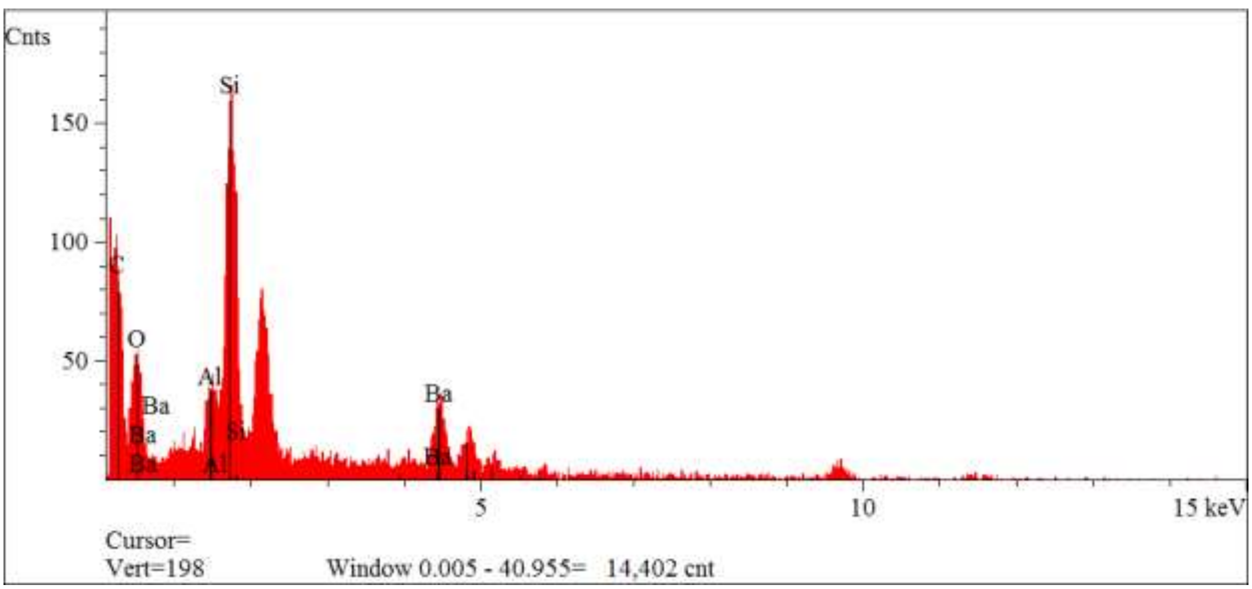

Spectrum 1

20C: Homogenous Filler Island: Peaks represent high concentrations

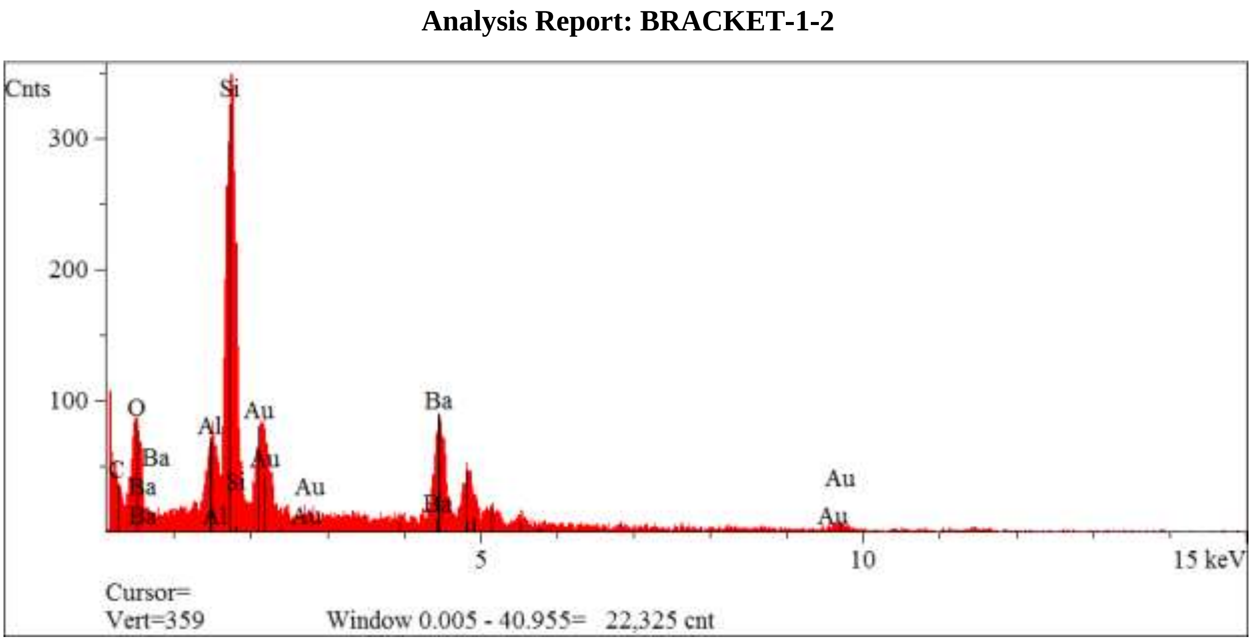

Spectrum 2